mPLUG-Owl3: Towards Long Image-Sequence Understanding in Multi-Modal Large Language Models

Anonymous authors
Paper under double-blind review

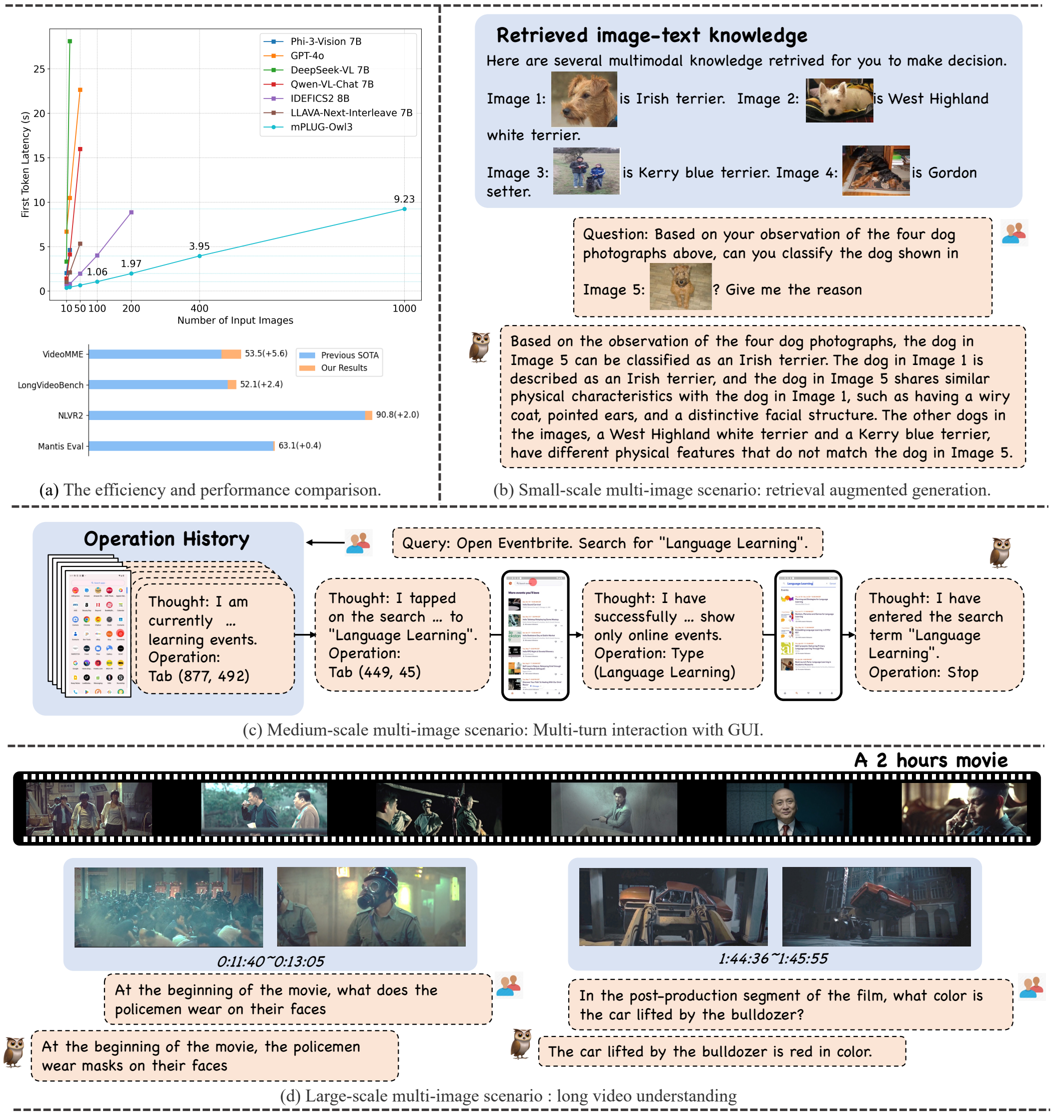

(a) The efficiency and performance comparison.

Retrieved image-text knowledge

Here are several multimodal knowledge retrived for you to make decision.

Image 1: is Irish terrier. Image 2: is West Highland white terrier.

Image 3: is Kerry blue terrier. Image 4: is Gordon setter.

Question: Based on your observation of the four dog photographs above, can you classify the dog shown in Image 5: ? Give me the reason

Based on the observation of the four dog photographs, the dog in Image 5 can be classified as an Irish terrier. The dog in Image 1 is described as an Irish terrier, and the dog in Image 5 shares similar physical characteristics with the dog in Image 1, such as having a wiry coat, pointed ears, and a distinctive facial structure. The other dogs in the images, a West Highland white terrier and a Kerry blue terrier, have different physical features that do not match the dog in Image 5.

(b) Small-scale multi-image scenario: retrieval augmented generation.

Operation History

Query: Open Eventbrite. Search for "Language Learning".

Thought: I am currently ... learning events.
Operation:
Tab (877, 492)

Thought: I tapped on the search ... to "Language Learning".
Operation:
Tab (449, 45)

Thought: I have successfully ... show only online events.
Operation: Type (Language Learning)

Thought: I have entered the search term "Language Learning".
Operation: Stop

(c) Medium-scale multi-image scenario: Multi-turn interaction with GUI.

A 2 hours movie

0:11:40~0:13:05

1:44:36~1:45:55

At the beginning of the movie, what does the policemen wear on their faces

At the beginning of the movie, the policemen wear masks on their faces

In the post-production segment of the film, what color is the car lifted by the bulldozer?

The car lifted by the bulldozer is red in color.

(d) Large-scale multi-image scenario : long video understanding

Figure 1: (a) mPLUG-Owl3 demonstrates leading performance on video and multi-image understanding. (b,c,d) Examples of mPLUG-Owl3 on handling different scale of multi-image scenarios.

Abstract

Multi-modal Large Language Models have demonstrated remarkable capabilities in executing instructions for a variety of single-image tasks. Despite this progress, significant challenges remain in modeling long image sequences. In this work, we introduce the versatile multi-modal large language model, mPLUG-Owl3, which enhances the capability for long image-sequence understanding in scenarios that incorporate retrieved image-text knowledge, multimodal in-context examples, and lengthy videos. Specifically, we propose novel hyper attention blocks to efficiently integrate vision and language into a common language-guided semantic space, thereby facilitating the processing of extended multi-image scenarios. We conduct evaluations on 21 benchmarks that cover single/multi-image, and short/long video understanding. mPLUG-Owl3 achieves competitive performance with the state-of-the-art methods while reducing inference time and memory usage by 87.8% and 48.5% in average. Moreover, we propose a Distractor Resistance evaluation to assess the ability of models to maintain focus amidst distractions. mPLUG-Owl3 also demonstrates outstanding performance in distractor resistance on ultra-long visual sequence inputs. We hope that mPLUG-Owl3 can contribute to the development of more efficient and powerful multimodal large language models.

1 Introduction

Recently, Multimodal Large Languages Models (Liu et al., 2023a; Ye et al., 2023b; Liu et al., 2024a; Ye et al., 2024; Chen et al., 2024d) have achieved rapid advancements, demonstrating strong single-image understanding capabilities. The current approaches primarily rely on vast amounts of image and text data to align Large Language Models (Zheng et al., 2023; Touvron et al., 2023a;b) with visual encoders, thereby extending multimodal capabilities.

More advanced image-sequence understanding capabilities are required in practical applications, such as Multi-Image Reasoning (Suhr et al., 2018; Lu et al., 2021; Jiang et al., 2024), Multimodal RAG (Chen et al., 2022; Lin et al., 2024), Video Understanding (Xiao et al., 2021; Li et al., 2023c; Fu et al., 2024a; Wu et al., 2024), Multi-modal Agents (Wang et al., 2024; Zhang et al., 2024a), and Multi-Doc QA (Tito et al., 2023; Van Landeghem et al., 2023). The existing methods are primarily based on interleaved image-text web data for pre-training (Laurençon et al., 2023; Laurençon et al., 2024) to extend multi-image capabilities or focused on the in-context abilities (Alayrac et al., 2022; Awadalla et al., 2023; Zhao et al., 2023) within multi-image scenarios. However, these methods have not explored the in-depth comprehension or the efficiency of multi-images sufficiently, which makes it hard to support long image sequences. For example, LLAVA-Next-Interleave (Li et al., 2024) and IDEFICS2 (Laurençon et al., 2024) insert raw or compressed visual features into textual sequences. As shown in Figure 1 (a), the inference latency increases dramatically as the number of images increases. This design also costs more memory and hinders these models from processing more visual inputs.

To address this challenge, we introduce mPLUG-Owl3, a new general-purpose multi-modal foundation model. mPLUG-Owl3 is designed to handle long image sequences both effectively and efficiently. mPLUG-Owl3 integrates innovative hyper attention blocks in the language model to achieve efficient interleaved vision-language semantic alignment. Specifically, Hyper Attention introduces cross-attention parallel to the self-attention in the transformer block. The language query is reused to select and extract visual features from a lengthy visual sequence, allowing for adaptively obtaining complementary visual information that the language model lacks, based on textual semantics.

As shown in Figure 1 (b,c,d), the mPLUG-Owl3, characterized by its high inference efficiency, is also capable of handling a variety of tasks involving interleaved text and image modalities, including multimodal retrieval-augmented generation, multimodal in-context examples, and long video understanding. mPLUG-Owl3 also can handle inputs containing up to 1,000 images at an extremely fast speed surpassing the existing models. We evaluate mPLUG-Owl3 with a total of twenty-one benchmarks, spanning single-image, multi-image, short, and long video scenarios. Among models of the 8B-level size training on publicly available data, mPLUG-Owl3 achieves state-of-the-art results in 15 out of 21 benchmarks. Besides existing benchmarks, we also propose a challenging long visual sequence evaluation named Distractor Resistance. It is designed to assess the ability of models to maintain focus amidst distractions. mPLUG-Owl3 demonstrates outstanding performance in handling ultra-long visual sequence inputs while also maintaining extremely high execution efficiency. It can also reduce inference time costs by 87.8% and memory usage by 48.5% in average compared to concatenate-based method. The superior performance of the new architecture in mPLUG-Owl3 implies a trend for future multimodal large language models.

2 mPLUG-Owl3

As illustrated in Figure 2, mPLUG-Owl3 comprises a visual encoder, a linear projection layer, and a decoder-only language model. This architecture is commonly employed in recently proposed Multi-modal Large Language Models. Unless specified otherwise, we use Siglip-400m (Zhai et al., 2023) as the visual encoder and Qwen2 (Yang et al., 2024) as the language model. First, we provide detailed information about our efficient architecture and its handling of various lengths of visual inputs in Section 2.1. Additionally, we introduce the Hyper Attention module in Section 2.2. It is a lightweight extension designed to enhance the transformer blocks of the language model by enabling cross-attention capabilities for adaptive visual sequence utilization.

2.1 Cross-Attention based Architecture

Popular MLLMs (e.g., LLAVA-Interleave (Li et al., 2024), InternVL (Chen et al., 2024d)) insert visual features into the sequence of embeddings, which can easily exhaust the language model's context window, resulting in significant memory and computational overhead. This kind of disadvantage hinders these MLLMs to modeling the long vision input such as multiple images, videos and multiple pieces high-resolution images.

Therefore, mPLUG-Owl3 consider use cross-attention for feeding the visual information into the language model. Specifically, given a interleaved multimodal input $S = [T_1, I_1, T_2, I_2, T_3]$ (the format can be adapted to various text-image organizational structures), mPLUG-Owl3 first extract visual features of the input images and use a linear projection to align the dimensions of visual features to be the same of the language model. The projected visual features are denoted by $\mathbf{H_{img}} = [I_1^t, I_2^t] \in \mathbb{R}^{L \times D_t}$. The text sequence are $S_{text} = [T_1, T_{img}, T_2, T_{img}, T_3] \in \mathbb{R}^{L \times D_t}$, where T_{img} is a plain text <|*image*|> to indicate the original place of the image. We feed the sequence into the word embedding to obtain text feature $\mathbf{H_{text}}$.

In the language model, we fuse the visual features $\mathbf{H_{img}}$ into the text features $\mathbf{H^i_{text}} \in \mathbb{R}^{L \times D_t}$ of the i^{th} layer through cross-attention operator. Different from Flamingo (Alayrac et al., 2022) and EVLM (Chen et al., 2024b) that insert an additional layer into each layer of transformer layer, we sparsely extend a small number of transformer blocks in the network to perform cross attention parallel with self-attention. We name this the Hyper Attention Transformer Block (HATB). We discuss the design of HATB in detail in Section 2.2. HABT can significantly reduces the number of additional training parameters and facilitates model convergence. Besides, we observe that having fewer HATBs does not degrade the model's performance; instead, it offers the advantages of low memory consumption and high inference efficiency during inference. For a language model consisting of N layers, we start from layer 0 and uniformly extend K layers to HATB.

2.2 Hyper Attention Transformer Block

In this section, we specifically introduce the Hyper Attention Transformer Block used in mPLUG-Owl3. The cross-attention structure employed in Flamingo, as shown in Figure 3 (a), has been widely utilized in constructing MLLMs (e.g., IDEFICS (Laurençon et al., 2023), EVLM (Chen et al., 2024b)). However, this structure presents three main drawbacks: it introduces a large number of additional parameters, which results in significant memory and computational overhead; the knowledge learned by the language model cannot benefit the understanding of visual inputs; the cross attention does not fully take into account the original positions of images in the interleaved sequence, which limits the performance of these models in multi-image scenarios. In response to these issues, we propose a lightweight Hyper Attention Transformer Block, illustrated in Figure 3 (b). This block introduces a small number of parameters and extends self-attention capabilities

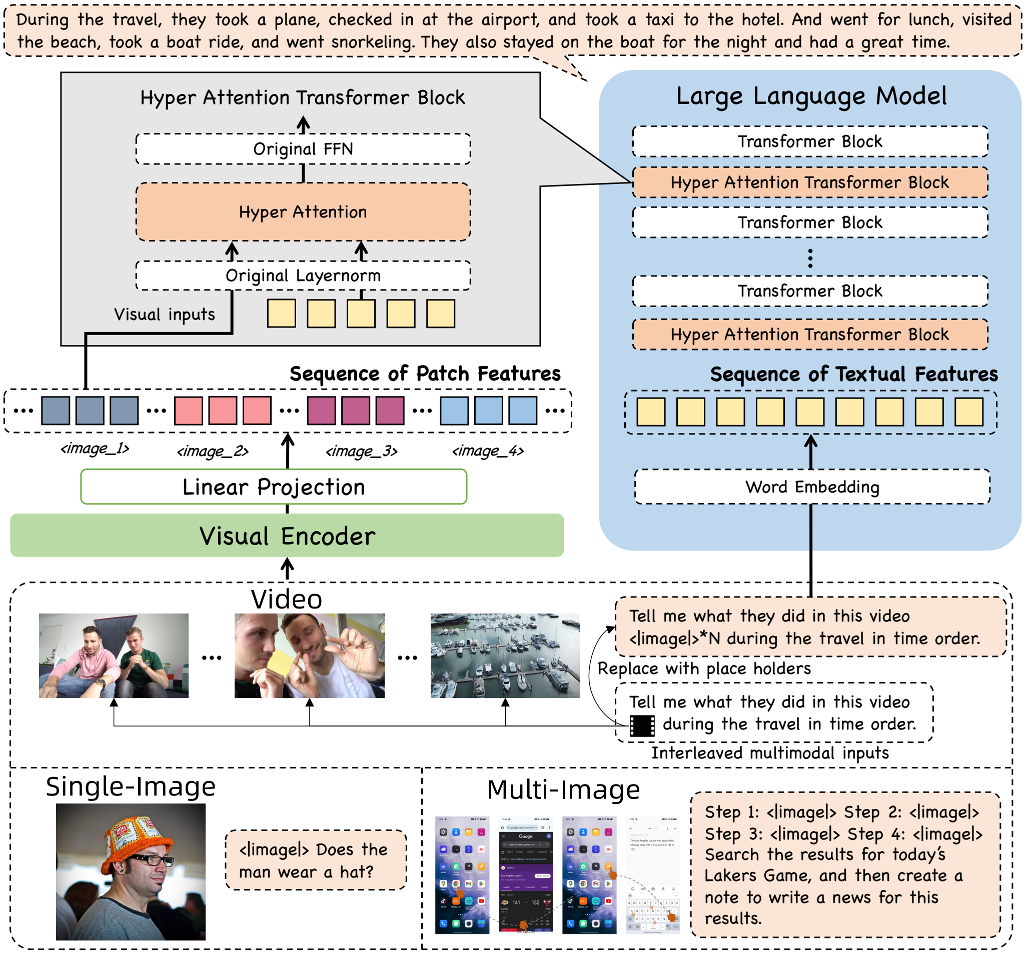
During the travel, they took a plane, checked in at the airport, and took a taxi to the hotel. And went for lunch, visited the beach, took a boat ride, and went snorkeling. They also stayed on the boat for the night and had a great time.
Hyper Attention Transformer Block
Original FFN
Hyper Attention
Original Layernorm
Visual inputs
Large Language Model
Transformer Block
Hyper Attention Transformer Block
Transformer Block
Transformer Block
Hyper Attention Transformer Block
Sequence of Patch Features
<image_1>
<image_2>
<image_3>
<image_4>
Sequence of Textual Features
Linear Projection
Visual Encoder
Word Embedding
Video
Tell me what they did in this video <|image|>*N during the travel in time order.
Replace with place holders
Tell me what they did in this video during the travel in time order.
Interleaved multimodal inputs
Single-Image
<|image|> Does the man wear a hat?
Multi-Image
Step 1: <|image|> Step 2: <|image|> Step 3: <|image|> Step 4: <|image|> Search the results for today's Lakers Game, and then create a note to write a news for this results.

Figure 2: An overview of mPLUG-Owl3.

to perform both intra-text self-attention and inter-modal cross-attention between text and images in parallel. It also introduces a Multimodal-Interleaved Rotary Position Embedding (MI-Rope) to maintain the position information of images. The extended modifications are detailed below:

Shared Input Layernorm. The visual feature $\mathbf{H_{img}}$ and the i^{th} layer's text features $\mathbf{H^{i}_{text}}$, although sharing the same dimensionality, originate from different distributions. Hence, both sets of features are initially normalized using a LayerNorm module. Our findings indicate that employing the LayerNorm module already integrated within the transformer block results in better convergence compared to training a separate layer normalization module specifically for the visual features.

Modality-Specific Key-Value Projection. In cross-attention, the **Query** is derived from textual data, while the **Key** and **Value** are extracted from visual features. Inspired by Ye et al. (2024), we construct a weight matrix $\mathbf{W}^{K\&V}_{img} \in \mathbb{R}^{2D\times D}$ to generate the **Key** and **Value** for the visual features. This matrix is initialized using the weights from the language model's KV (Key-Value) projection. Furthermore, the query vector from the self-attention mechanism is repurposed as the **Query** in the cross-attention. The computation procedure for self-attention remains unchanged. This design is beneficial as it preserves more specific visual information and allows for the adaptive supplementation of visual information that the language model lacks, based on textual semantics.

Visual Position Modeling in Attention. For models that process multiple images, positional encoding is essential to correctly understanding interleaved image-text input. Existing cross-attention models, such as Flamingo (Alayrac et al., 2022) and IDEFICS (Laurençon et al., 2023), do not assign

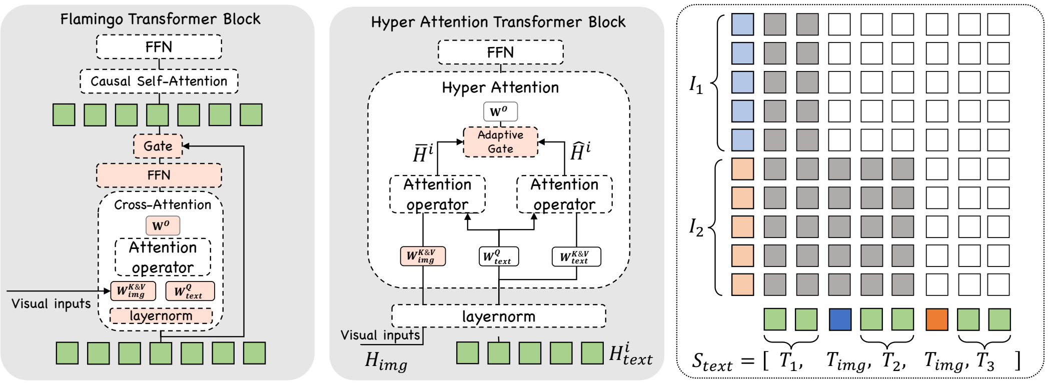

(a) Flamingo Transformer Block (b) Hyper Attention Transformer Block (c) Causal Attention Mask of Cross-Attention

Figure 3: Comparison between Flamingo Transformer Block (a) and Hyper Attention Transformer Block (b). Pink indicates that the module is additionally introduced. (c) presents the causal attention mask strategy of cross attention in Hyper Attention in a image-text interleaved scenario. The gray block denotes the attention score is ignored. T_{img} denotes the token of plain text <|*image*|>.

position embeddings to visual inputs, leading to suboptimal performance in scenarios involving multiple images. To accurately represent the original positions of images in interleaved sequences, we develope a Multimodal-Interleaved Rotary Position Embedding, which we name MI-Rope. Specifically, for each visual feature I_n of image n, we pre-record the position index of its placeholder T_{img} in the interleaved sequence S_{text}. All patches of I_n share T_n's positional encoding to obtain the rotary embedding. This ensures that the positional encoding of the image not only reflects the order among images but also reveals its position in the textual context. We also use a causal attention mask in cross attention. As shown in Figure 3 (c), for a text sequence $S = [T_1, T_{img}, T_2, T_{img}, T_3]$, each text token can only attend the visual features that precede it. Then, HATB simultaneously performs cross-attention and self-attention, denoting the resulting hidden states as $\bar{\mathbf{H}}^{\mathbf{i}}$ and $\hat{\mathbf{H}}^{\mathbf{i}}$.

Adaptive Gating Existing implementations of cross-attention utilize a learnable scale to regulate the extent of information transfer from the image to the language model. However, the semantics of language are ignored. Consequently, we introduce an adaptive gate that obtains the gate value based on the textual features. Gate value of each token is obtained by: $\mathbf{g} = \text{Sigmoid}(\mathbf{W}_{gate}^{T}\hat{\mathbf{H}}^{\mathbf{i}})$. Then, the multimodal features are fused: $\mathbf{H}^{\mathbf{i}}_{\mathbf{fused}} = \bar{\mathbf{H}}^{\mathbf{i}}_{\mathbf{text}} * \mathbf{g} + \hat{\mathbf{H}}^{\mathbf{i}}_{\mathbf{text}} * (1 - \mathbf{g})$. The $\mathbf{H}^{\mathbf{i}}_{\mathbf{fused}}$ is passed to the FFN and fed to the next layer of transformer.

3 Implement Details

3.1 Training Paradigm

We adopt a three-stage training approach for mPLUG-Owl3. Initially, we pre-train mPLUG-Owl3 using image-text pairs to achieve robust multimodal alignment. In the second stage, we leverage diverse datasets that include image and video captions to enhance the model's ability to understand multiple images. Finally, we fine-tune mPLUG-Owl3 using a mixture of supervised data, encompassing tasks involving both single and multiple images, to ensure comprehensive performance. The statistics of the datasets, the training settings and data processing details can be found in Appendix A. We train three sizes of mPLUG-Owl3, based on Qwen2 with sizes of 0.5B, 1.5B, and 7B. All three models share the same visual encoder.

3.1.1 Pre-training

We follow the mPLUG-Owl2 (Ye et al., 2024) to collect the pre-training datasets and randomly sample a subset consists of 41 million image-text pairs for pre-training. During pre-training, only the newly introduced modules are trainable, which include the linear layer following the vision encoder, the visual KV projection, and the Adaptive Gate in the Hyper Attention Transformer Block.

Model	# Param	VQAv2	OK-VQA	GQA	VizWizQA	TextVQA
CogVLM	17B	82.3	64.8	-	-	70.4
EVLM-Chat	32B	81.9	-	64.4	47.3	67.5
Flamingo	80B	81.3	50.6	-	57.2	54.7
8B-level MLLMs						
Idefics1	9B	68.8	50.4	-	-	39.3
Flamingo	9B	51.8	44.7	-	-	46.3
mPLUG-Owl2	8B	79.4	57.7	56.1	54.5	58.2
LLAVA-1.5	8B	78.5	-	62.0	50.0	58.2
LLAVA-Next	8B	81.8	-	64.2	57.6	64.9
VILA-1.5	8B	80.9	-	61.9	58.7	66.3
Idefics2	8B	80.8	53.5	51.1	58.5	**70.4**
Mantis-SigLIP	8B	74.9	55.4	56.3	42.2	59.2
mPLUG-Owl3	1B	69.2	40.3	55.7	34.8	53.1
	2B	79.3	53.2	61.0	56.6	62.6
	8B	**82.1**	**60.1**	**65.0**	**63.5**	69.0

Table 1: **Performance comparison on visual question answering.** The accuracy is reported. We use **bold** to mark the highest score and underline to mark the second highest of 8B-level MLLMs.

3.1.2 Multi-image Pre-training

In the multi-image pre-training stage, we collected three types of data to enhance the model's multi-image understanding capabilities: (1) Interleaved data. We utilize sources such as MMDU (Liu et al., 2024c) and M4-Instruction (Li et al., 2024) for multi-image data. Additionally, from LLaVA-Recap 558K, we randomly sample 3 to 6 images and combine their image-caption pairs into an interleaved format to create Interleaved Captions. We also consider sampling 4 images and requiring a description of one among them to form Selective Captions. (2) Text-rich data. We use text reading and key point generation data proposed by UReader (Ye et al., 2023a), enabling the model to reconstruct the text and extract key points contained within text-rich images. (3) Video data. We adopt annotated data from ShareGPTVideo (Zhang et al., 2024b), which includes 900K caption entries and 240K question-answering instances. We also incorporate Chinese and English video caption data from VATEX (Wang et al., 2019). During multi-image training, modules except visual transformer are trainable.

3.1.3 Supervised-Finetuning

In Supervised-Finetuning stage, mPLUG-Owl3 is trained with an extensive and diverse assembly of instruction tuning datasets aimed at enhancing its instruction-following capability. The datasets include LLaVA-SFT-665K (Liu et al., 2024a), The Cauldron (Laurençon et al., 2024), Mantis (Jiang et al., 2024), M4-Instruction (Li et al., 2024), ALLaVA (Chen et al., 2024a), ShareGPTVideo-QA 240K (Zhang et al., 2024b), Video Instruct 100K (Maaz et al., 2023), MSR-VTT (Xu et al., 2016) and MSVD Caption (Chen & Dolan, 2011). We keep the same training setting as the Multi-image Pre-training stage.

4 Experiments

4.1 Visual Question Answering Benchmarks

We conduct experiments on VQAv2 (Goyal et al., 2016), OK-VQA (Marino et al., 2019), GQA (Hudson & Manning, 2019), VizWizQA (Bigham et al., 2010), and TextVQA (Singh et al., 2019). The detail introduction can be found in Appendix H.1. These datasets are strategically selected to thoroughly evaluate our model's ability to understand and reason across various visual contexts and knowledge domains.

Table 1 presents the comparison results between mPLUG-Owl3 and State-of-the-Art multimodal large language models trained on publicly available data. mPLUG-Owl3 outperforms 8B-level language models in VQAv2, OK-VQA, GQA, and VizWizQA. Furthermore, it surpasses the 32B-

Model	# Param	MMB-EN	MMB-CN	MM-Vet	POPE	AI2D
CogVLM	17B	65.8	69.8	52.8	88.0	63.3
EVLM-Chat	32B	76.9	76.9	-	89.7	76.0
8B-level MLLMs						
LLAVA-1.5	8B	64.3	58.3	31.1	85.9	55.5
OpenFlamingo	9B	32.4	14.4	24.8	-	31.7
mPLUG-Owl2	8B	64.5	-	36.2	-	55.7
LLAVA-Next	8B	67.4	60.6	43.9	86.5	66.6
LLAVA-Interleave	8B	-	-	39.1	86.8	73.9
VILA1.5	8B	72.3	66.2	38.3	84.4	-
Idefics2	8B	75.7	68.6	34.0	86.2	72.3
Cambrian	8B	74.6	67.9	**48.1**	86.4	**74.6**
Mantis-SigLIP	8B	68.7	63.1	39.3	84.5	67.3
mPLUG-Owl3	1B	51.4	44.8	21.4	85.3	46.7
	2B	65.7	61.8	36.3	87.4	62.6
	8B	**77.6**	**74.3**	40.1	**88.2**	73.8

Table 2: **Zero-shot multi-modal evaluation on multi-modal benchmarks.** The overall scores are reported for evaluation. We use **bold** to mark the highest score and underline to mark the second highest of 8B-level MLLMs.

parameter EVLM in GQA and VizWizQA. In TextVQA, although mPLUG-Owl3's performance is slightly lower than that of Idefics2, it still exceeds that of other 8B models. It is noteworthy that, despite having 8B parameters, mPLUG-Owl3 exhibits superior inference speed and memory efficiency compared to models of the same scale, thanks to the introduction of Hyper Attention.

4.2 General MLLM Benchmarks

We evaluate mPLUG-Owl3 on various single-image general multimodal large language model benchmarks including MMBench (Liu et al., 2023b), MM-Vet (Yu et al., 2023), POPE (Li et al., 2023d) and AI2D (Kembhavi et al., 2016). Please refer to the Appendix H.1 for more details.

Table 2 shows that mPLUG-Owl3 achieves state-of-the-art performance on MMBench-EN, MMBench-CN, MM-Vet and POPE across 8B-level models. It also matches or surpasses the performance of larger models such as CogVLM (Wang et al., 2023) and EVLM-Chat (Chen et al., 2024b). mPLUG-Owl3 does not achieve state-of-the-art performance on the AI2D dataset. Due to limited training resources, we do not fine-tune the vision encoder, which restricts its performance in scenarios rich in text.

4.3 Multi-image and Video Benchmark

We also evaluate the performance of mPLUG-Owl3 on video and multi-image benchmarks (including NextQA (Xiao et al., 2021), MVBench (Li et al., 2023c) VideoMME (Fu et al., 2024a), LongVideoBench (Wu et al., 2024) and MLVU (Zhou et al., 2024)), as it is capable of processing multiple images with an interleaved format. The introduction of benchmakrs and sample setting can be found in Appendix H.2.

The results of video evaluation is shown in Table 3. On benchmark that measure the short video understanding performance, mPLUG-Owl3 achieves performance comparable to state-of-the-art models. And on long video benchmarks, mPLUG-Owl3 significantly outperforms existing models and present a more significant advantage in understanding long videos. The results demonstrates that mPLUG-Owl3 is highly suitable for understanding videos with various durations. We also present qualitative results on video understanding in Appendix G.2.

Table 4 presents the the evaluation results on multi-image understanding. The evaluation benchmarks consist of NLVR2 (Suhr et al., 2018), Mantis-Eval (Jiang et al., 2024), MathVerse-mv (Li et al., 2024), SciVerse-mv (Li et al., 2024), BLINK (Fu et al., 2024b) and Q-Bench2 (Zhang et al., 2024c)). We provide a detail introduction in Appendix H.3.

Model	# Param	NextQA	MVBench	VideoMME w/o sub	LongVideoBench-val	MLVU
VideoChat2	8B	68.6	51.9	43.8	36.0	47.9
Video-LLaMA2	8B	-	**54.6**	47.9	-	48.5
Video-ChatGPT	8B	-	32.7	-	-	31.3
ShareGPT4Video	8B	-	-	39.9	39.7	46.4
PLLaVA	8B	-	46.6	-	40.2	-
Idefics2	8B	-	29.7	25.9	49.7	49.8
Mantis-SigLIP	8B	-	50.2	44.0	47.0	49.3
LLAVA-Interleave	8B	78.2	53.1	48.7	48.8	56.4
mPLUG-Owl3	1B	65.3	47.1	41.8	42.8	52.7
	2B	74.5	51.8	48.4	50.4	59.8
	8B	**78.6**	54.5	**53.5**	**52.1**	**63.7**

Table 3: **Multi-modal evaluation on video understanding benchmarks.** The overall scores are reported for evaluation. We use **bold** to mark the highest score and underline to mark the second highest.

mPLUG-Owl3 surpasses existing models in both NLVR2 and Mantis-Eval. On MathVerse-mv and SciVerse-mv, it can be observed that mPLUG-Owl3 significantly outperforms LLaVA-Interleave. However, on BLINK, mPLUG-Owl3 performs weaker than LLaVA-Interleave. We note that this dataset requires models to possess low-level visual perception capabilities for fine details in images, and mPLUG-Owl3's ability may be limited due to the vision encoder being frozen during training. On the Q-Bench2, which evaluates a model's ability to discern low-level visual differences across multiple images globally, mPLUG-Owl3 achieves performance comparable to the state-of-the-art. We also conduct fine-grained multi-image experiments and present the result in Appendices B and C. mPLUG-Owl3 exhibits a stronger capability for following external multimodal knowledge. Additionally, we also present qualitative results of the multi-image understanding scenarios in Appendix G.1.

Model	# Param	NLVR2	Mantis-Eval	MathVerse-mv	SciVerse-mv	BLINK	Q-Bench2
CogVLM	17B	58.6	45.2	-	-	41.5	53.2
VideoLLaVA	8B	56.5	35.9	-	-	38.9	45.7
VILA	8B	76.5	51.2	-	-	39.3	45.7
Idefics2	8B	86.9	48.9	-	-	45.2	57.0
Mantis-SigLIP	8B	87.4	59.5	-	-	46.4	69.9
LLAVA-Interleave	8B	88.8	62.7	32.8	31.6	**52.6**	**74.2**
mPLUG-Owl3	1B	75.8	39.6	23.9	26.4	40.6	50.6
	2B	85.5	54.4	42.5	30.0	43.0	65.8
	8B	**90.8**	**63.1**	**65.0**	**86.2**	50.3	74.0

Table 4: **Multi-modal evaluation on multi-image understanding benchmarks.** The overall scores are reported for evaluation. We use **bold** to mark the highest score and underline to mark the second highest.

4.4 Ablation Studies

In this section, we investigate the integration method and design of Hyper Attention. We also validate the integration density and the results are presented in Appendix E. For ablation study experiments, we adopt the training methods of LLaVA-1.5 (Liu et al., 2024a) using the same datasets to conduct our ablation study. Additionally, we employ the Qwen1.5 7B as our language model. To validate the single-image understanding capabilities of our structures, we use datasets such as GQA and TextVQA (with OCR). We conducti zero-shot evaluations on benchmarks including MvBench, VideoMME, NLVR2, and Mantis-Eval to examine the generalization capabilities in multi-image understanding and video comprehension.

4.4.1 Cross Attention Integration

There are two primary methods to integrate Cross-Attention into the transformer block: one method positions it prior to the self-attention (referred to as Pre-Cross-Attention), while the other places it

Attention Structure	Elapsed Time (ms)	VRAM (GB)	GQA	TextVQA	MvBench	VideoMME	NLVR2	Mantis-Eval
Concatenate	2761.7	40.6	**59.0**	**51.6**	22.4	25.1	55.7	38.7
Pre-Cross-Attention	384.3	21.2	53.8	45.2	**43.0**	38.9	55.3	44.7
Post-Cross-Attention	397.2	21.2	48.9	40.9	38.3	37.0	54.0	47.0
Hyper Attention	**336.9**	**20.9**	57.6	50.0	42.8	**39.4**	**59.5**	**51.6**

Table 5: Comparison between different attention structure. Concatenate means direct concatenate visual and text feature sequences. We use **bold** to mark the highest score.

Adaptive Gating	Shared LayerNorm	MI-Rope	GQA	TextVQA	MvBench	VideoMME	NLVR2	Mantis
			53.3	44.6	40.2	38.1	52.7	41.9
✓			55.7	49.3	**43.2**	**40.1**	53.4	47.9
✓	✓		**58.1**	49.7	42.8	38.4	54.9	46.1
✓	✓	✓	57.6	**50.0**	42.8	39.4	**59.5**	**51.6**

Table 6: Ablation on the Adaptive Gating, Shared LayerNorm and MI-Rope.

subsequent to the self-attention (referred to as Post-Cross-Attention). We analyze both configurations and compare them to the concatenate-based method and our novel Hyper Attention in mPLUG-Owl3.

Table 5 shows that the concatenate-based model which directly embeds image features into the input sequence of the language model, has the best performance in single-image understanding. On the other hand, utilizing Post-Cross-Attention results in the worst performance. Comparatively, Pre-Cross-Attention performs better but still incurs some performance loss. Hyper Attention, however, achieves comparable performance with concatenate-based model. In evaluations involving videos and multiple images, we observe that the concatenate-based model demonstrate poor performance. This is attributed to the inadequate training of inter-image attention, which significantly disrupts the model's hidden states. Conversely, both single images and multiple images share the same paradigm when performing cross attention with text, which allows its multi-image capability to be better generalized from single-image training. the Hyper Attention design stands out as particularly effective in balancing the model's capabilities for handling both single and multiple images, showcasing superior generalizability. It also reduces inference time costs by 87.8% and memory usage by 48.5% in average compared to concatenate-based method.

4.4.2 Design of Hyper Attention

To further investigate the impact of the structural design of Hyper Attention on model performance, we start with a basic hyper attention model and gradually introduce adaptive gating, shared layernorm, and MI-Rope. The Table 6 shows that when incorporate adaptive gating, the single-image understanding performance is significantly improved. And if we use a shared layernorm, performance is further improved. In video scenario, we notice that even without any inter-image position encoding, the performance of video understanding is also improved, suggesting the temporality inherent in visual content can also be implicitly modeled by the model with the help of adaptive gating. However, when evaluating models with multiple images, the contextual position of the images is crucial and cannot be implicitly modeled. Therefore, it can be observed that incorporating adaptive gating and shared layernorm does not lead to performance improvement on multi-image benchmarks. However, with the introduction of MI-Rope, the metrics for various multi-image benchmarks have demonstrated significant improvement.

4.5 Distractor Resistance in Long Visual Contexts

We develop a challenge evaluation method to assess the distractor resistance of multimodal models in long visual contexts. Specifically, based on MMBench, we randomly insert N Distractor images, where $N = 1, 5, 10, 20, 50, 100, 200, 400$ and measure the model's accuracy. The details of the experiment setting and analysis can be found in Appendix D.

In Figure 4, LLaVA and Mantis struggles to consistently answer the questions accurately when 50 distractors images are present, resulting in a low accuracy rate. In contrast, mPLUG-Owl3 only drops to a performance level of 43.09%. As the images increases to 400, the performance of mPLUG-Owl3 decreases to 28.58%. It is still a challenging task and valuable for future models to evaluate.

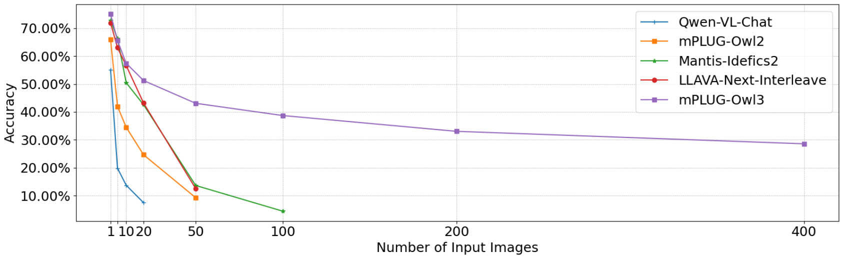

Figure 4: The performance of interference resistance with long visual context across LLaVA-Next-Interleave 7B, Mantis-Idefics2, Qwen-VL, mPLUG-Owl2 and mPLUG-Owl3.

5 Related Work

5.1 Multimodal Large Language Models

Multimodal large language models (MLLMs) can perceive visual contents, conduct visual reasoning, and engage in multimodal dialogue with humans.

Models like LLaVA (Liu et al., 2023a) use an MLP to map visual features into the representation space of the language model, and directly concatenate them with the text sequence. These methods can preserve fine-grained visual information but consume a large number of tokens which slows down both training and inference. To reduce the number of tokens, models such as mPLUG-Owl (Ye et al., 2023b) and IDEFICS2 (Laurençon et al., 2024) adopt a structure similar to Q-Former (Li et al., 2023a), compressing the token count to a fixed size. Flamingo (Alayrac et al., 2022) first proposed embedding cross-attention layers into the language model, integrating visual features into the intermediate representations of the language model. IDEFICS (Laurençon et al., 2023) and EVLM (Chen et al., 2024b) have also trained MLLMs based on this structure. This method avoids occupying the context window of the LLM. However, it introduces more parameters and may interfere with the intermediate representations of the pre-trained language models, making the performance of such models often sub-optimal compared to mainstream models.

5.2 Multimodal Models with Interleaved Support

Recent research are expanding the capabilities of multimodal models to process multiple images inputs.

Video is a special form of multi-image existence, and MLLMs related to video understanding treat frames as multiple images with temporal correlation as input. These models such as VideoChat2 (Li et al., 2023b) and VideoLLaMA2 (Cheng et al., 2024) introduce extra module to compress temporal frames. ShareGPT4Video (Chen et al., 2024c) proposes to improve the video understanding by introducing GPT-4 annotated video caption as pretrain data. In general multi-image scenario, including in-context learning, cross image reference, comparison, and reasoning. Flamingo (Alayrac et al., 2022) demonstrates limited in-context learning capabilities, while Idefics2 (Laurençon et al., 2024) and LLAVA-Interleave (Li et al., 2024) further enhance the model's multi-image understanding capabilities by constructing more refined multi-image training data.

6 Conclusion

In this paper, we present mPLUG-Owl3, a multi-modal large language model that significantly advances the state-of-the-art in handling both single-image, multi-image and video tasks. The introduction of novel Hyper Attention enables the mPLUG-Owl3 to maintain the fine-grained visual input and effectively fuse visual and textual information, leading to superior performance across various benchmarks. We also propose a challenging long visual sequence evaluation named Distractor Resistance. Notably, mPLUG-Owl3 excels in managing ultra-long visual sequences and demonstrates a strong performance in evaluation. We believe that mPLUG-Owl3 reveals a direction for building efficient and effective multi-modal large language models.

References

Jean-Baptiste Alayrac, Jeff Donahue, Pauline Luc, Antoine Miech, Iain Barr, Yana Hasson, Karel Lenc, Arthur Mensch, Katherine Millican, Malcolm Reynolds, et al. Flamingo: a visual language model for few-shot learning. *Advances in Neural Information Processing Systems*, 35:23716–23736, 2022. 2, 3, 4, 10

Anas Awadalla, Irena Gao, Josh Gardner, Jack Hessel, Yusuf Hanafy, Wanrong Zhu, Kalyani Marathe, Yonatan Bitton, Samir Gadre, Shiori Sagawa, et al. Openflamingo: An open-source framework for training large autoregressive vision-language models. *arXiv preprint arXiv:2308.01390*, 2023. 2

Jeffrey P Bigham, Chandrika Jayant, Hanjie Ji, Greg Little, Andrew Miller, Robert C Miller, Robin Miller, Aubrey Tatarowicz, Brandyn White, Samual White, et al. Vizwiz: nearly real-time answers to visual questions. In *Proceedings of the 23nd annual ACM symposium on User interface software and technology*, pp. 333–342, 2010. 6, 20

David Chen and William B Dolan. Collecting highly parallel data for paraphrase evaluation. In *Proceedings of the 49th annual meeting of the association for computational linguistics: human language technologies*, pp. 190–200, 2011. 6

Guiming Hardy Chen, Shunian Chen, Ruifei Zhang, Junying Chen, Xiangbo Wu, Zhiyi Zhang, Zhihong Chen, Jianquan Li, Xiang Wan, and Benyou Wang. Allava: Harnessing gpt4v-synthesized data for a lite vision-language model. *arXiv preprint arXiv:2402.11684*, 2024a. 6

Kaibing Chen, Dong Shen, Hanwen Zhong, Huasong Zhong, Kui Xia, Di Xu, Wei Yuan, Yifei Hu, Bin Wen, Tianke Zhang, et al. Evlm: An efficient vision-language model for visual understanding. *arXiv preprint arXiv:2407.14177*, 2024b. 3, 7, 10

Lin Chen, Xilin Wei, Jinsong Li, Xiaoyi Dong, Pan Zhang, Yuhang Zang, Zehui Chen, Haodong Duan, Bin Lin, Zhenyu Tang, et al. Sharegpt4video: Improving video understanding and generation with better captions. *arXiv preprint arXiv:2406.04325*, 2024c. 10

Wenhu Chen, Hexiang Hu, Xi Chen, Pat Verga, and William W Cohen. Murag: Multimodal retrieval-augmented generator for open question answering over images and text. *arXiv preprint arXiv:2210.02928*, 2022. 2

Zhe Chen, Jiannan Wu, Wenhai Wang, Weijie Su, Guo Chen, Sen Xing, Muyan Zhong, Qinglong Zhang, Xizhou Zhu, Lewei Lu, et al. Internvl: Scaling up vision foundation models and aligning for generic visual-linguistic tasks. In *Proceedings of the IEEE/CVF Conference on Computer Vision and Pattern Recognition*, pp. 24185–24198, 2024d. 2, 3

Zesen Cheng, Sicong Leng, Hang Zhang, Yifei Xin, Xin Li, Guanzheng Chen, Yongxin Zhu, Wenqi Zhang, Ziyang Luo, Deli Zhao, et al. Videollama 2: Advancing spatial-temporal modeling and audio understanding in video-llms. *arXiv preprint arXiv:2406.07476*, 2024. 10

Chaoyou Fu, Yuhan Dai, Yondong Luo, Lei Li, Shuhuai Ren, Renrui Zhang, Zihan Wang, Chenyu Zhou, Yunhang Shen, Mengdan Zhang, et al. Video-mme: The first-ever comprehensive evaluation benchmark of multi-modal llms in video analysis. *arXiv preprint arXiv:2405.21075*, 2024a. 2, 7, 21

Xingyu Fu, Yushi Hu, Bangzheng Li, Yu Feng, Haoyu Wang, Xudong Lin, Dan Roth, Noah A. Smith, Wei-Chiu Ma, and Ranjay Krishna. Blink: Multimodal large language models can see but not perceive, 2024b. 7, 22

Yash Goyal, Tejas Khot, Douglas Summers-Stay, Dhruv Batra, and Devi Parikh. Making the v in vqa matter: Elevating the role of image understanding in visual question answering. *International Journal of Computer Vision*, 127:398 – 414, 2016. URL https://api.semanticscholar.org/CorpusID:8081284. 6, 20

Drew A Hudson and Christopher D Manning. Gqa: A new dataset for real-world visual reasoning and compositional question answering. In *Proceedings of the IEEE/CVF conference on computer vision and pattern recognition*, pp. 6700–6709, 2019. 6, 20

Dongfu Jiang, Xuan He, Huaye Zeng, Cong Wei, Max Ku, Qian Liu, and Wenhu Chen. Mantis: Interleaved multi-image instruction tuning. *arXiv preprint arXiv:2405.01483*, 2024. 2, 6, 7, 22

Aniruddha Kembhavi, Mike Salvato, Eric Kolve, Minjoon Seo, Hannaneh Hajishirzi, and Ali Farhadi. A diagram is worth a dozen images. In *Computer Vision–ECCV 2016: 14th European Conference, Amsterdam, The Netherlands, October 11–14, 2016, Proceedings, Part IV 14*, pp. 235–251. Springer, 2016. 7, 20

Hugo Laurençon, Léo Tronchon, Matthieu Cord, and Victor Sanh. What matters when building vision-language models? *arXiv preprint arXiv:2405.02246*, 2024. 2, 6, 10

Hugo Laurençon, Lucile Saulnier, Léo Tronchon, Stas Bekman, Amanpreet Singh, Anton Lozhkov, Thomas Wang, Siddharth Karamcheti, Alexander M. Rush, Douwe Kiela, Matthieu Cord, and Victor Sanh. Obelics: An open web-scale filtered dataset of interleaved image-text documents, 2023. 2, 3, 4, 10

Feng Li, Renrui Zhang, Hao Zhang, Yuanhan Zhang, Bo Li, Wei Li, Zejun Ma, and Chunyuan Li. Llava-next-interleave: Tackling multi-image, video, and 3d in large multimodal models. *arXiv preprint arXiv:2407.07895*, 2024. 2, 3, 6, 7, 10, 22

Junnan Li, Dongxu Li, Silvio Savarese, and Steven C. H. Hoi. Blip-2: Bootstrapping language-image pre-training with frozen image encoders and large language models. *ArXiv*, abs/2301.12597, 2023a. URL https://api.semanticscholar.org/CorpusID:256390509. 10

KunChang Li, Yinan He, Yi Wang, Yizhuo Li, Wenhai Wang, Ping Luo, Yali Wang, Limin Wang, and Yu Qiao. Videochat: Chat-centric video understanding. *arXiv preprint arXiv:2305.06355*, 2023b. 10

Kunchang Li, Yali Wang, Yinan He, Yizhuo Li, Yi Wang, Yi Liu, Zun Wang, Jilan Xu, Guo Chen, Ping Luo, Limin Wang, and Yu Qiao. Mvbench: A comprehensive multi-modal video understanding benchmark. *ArXiv*, abs/2311.17005, 2023c. URL https://api.semanticscholar.org/CorpusID:265466214. 2, 7, 21

Yifan Li, Yifan Du, Kun Zhou, Jinpeng Wang, Wayne Xin Zhao, and Ji rong Wen. Evaluating object hallucination in large vision-language models. *ArXiv*, abs/2305.10355, 2023d. URL https://api.semanticscholar.org/CorpusID:258740697. 7, 20

Weizhe Lin, Jinghong Chen, Jingbiao Mei, Alexandru Coca, and Bill Byrne. Fine-grained late-interaction multi-modal retrieval for retrieval augmented visual question answering. *Advances in Neural Information Processing Systems*, 36, 2024. 2

Haotian Liu, Chunyuan Li, Qingyang Wu, and Yong Jae Lee. Visual instruction tuning. *ArXiv*, abs/2304.08485, 2023a. URL https://api.semanticscholar.org/CorpusID:258179774. 2, 10

Haotian Liu, Chunyuan Li, Yuheng Li, and Yong Jae Lee. Improved baselines with visual instruction tuning. In *Proceedings of the IEEE/CVF Conference on Computer Vision and Pattern Recognition*, pp. 26296–26306, 2024a. 2, 6, 8

Haowei Liu, Xi Zhang, Haiyang Xu, Yaya Shi, Chaoya Jiang, Ming Yan, Ji Zhang, Fei Huang, Chunfeng Yuan, Bing Li, et al. Mibench: Evaluating multimodal large language models over multiple images. *arXiv preprint arXiv:2407.15272*, 2024b. 15, 16

Yuan Liu, Haodong Duan, Yuanhan Zhang, Bo Li, Songyang Zhang, Wangbo Zhao, Yike Yuan, Jiaqi Wang, Conghui He, Ziwei Liu, et al. Mmbench: Is your multi-modal model an all-around player? *arXiv preprint arXiv:2307.06281*, 2023b. 7, 20

Ziyu Liu, Tao Chu, Yuhang Zang, Xilin Wei, Xiaoyi Dong, Pan Zhang, Zijian Liang, Yuanjun Xiong, Yu Qiao, Dahua Lin, et al. Mmdu: A multi-turn multi-image dialog understanding benchmark and instruction-tuning dataset for lvlms. *arXiv preprint arXiv:2406.11833*, 2024c. 6

Pan Lu, Liang Qiu, Jiaqi Chen, Tony Xia, Yizhou Zhao, Wei Zhang, Zhou Yu, Xiaodan Liang, and Song-Chun Zhu. Iconqa: A new benchmark for abstract diagram understanding and visual language reasoning. *arXiv preprint arXiv:2110.13214*, 2021. 2

Muhammad Maaz, Hanoona Rasheed, Salman Khan, and Fahad Shahbaz Khan. Video-chatgpt: Towards detailed video understanding via large vision and language models. *ArXiv*, abs/2306.05424, 2023. URL https://api.semanticscholar.org/CorpusID:259108333. 6

Kenneth Marino, Mohammad Rastegari, Ali Farhadi, and Roozbeh Mottaghi. Ok-vqa: A visual question answering benchmark requiring external knowledge. In *Proceedings of the IEEE/cvf conference on computer vision and pattern recognition*, pp. 3195–3204, 2019. 6, 20

Amanpreet Singh, Vivek Natarajan, Meet Shah, Yu Jiang, Xinlei Chen, Dhruv Batra, Devi Parikh, and Marcus Rohrbach. Towards vqa models that can read. In *Proceedings of the IEEE/CVF conference on computer vision and pattern recognition*, pp. 8317–8326, 2019. 6, 20

Alane Suhr, Stephanie Zhou, Iris Zhang, Huajun Bai, and Yoav Artzi. A corpus for reasoning about natural language grounded in photographs. *ArXiv*, abs/1811.00491, 2018. URL https://api.semanticscholar.org/CorpusID:53178856. 2, 7, 22

Rubèn Tito, Dimosthenis Karatzas, and Ernest Valveny. Hierarchical multimodal transformers for multipage docvqa. *Pattern Recognition*, 144:109834, 2023. 2

Hugo Touvron, Thibaut Lavril, Gautier Izacard, Xavier Martinet, Marie-Anne Lachaux, Timothée Lacroix, Baptiste Rozière, Naman Goyal, Eric Hambro, Faisal Azhar, Aurelien Rodriguez, Armand Joulin, Edouard Grave, and Guillaume Lample. Llama: Open and efficient foundation language models. *ArXiv*, abs/2302.13971, 2023a. URL https://api.semanticscholar.org/CorpusID:257219404. 2

Hugo Touvron, Louis Martin, Kevin R. Stone, Peter Albert, Amjad Almahairi, Yasmine Babaei, Nikolay Bashlykov, Soumya Batra, Prajjwal Bhargava, Shruti Bhosale, Daniel M. Bikel, Lukas Blecher, Cristian Cantón Ferrer, Moya Chen, Guillem Cucurull, David Esiobu, Jude Fernandes, Jeremy Fu, Wenyin Fu, Brian Fuller, Cynthia Gao, Vedanuj Goswami, Naman Goyal, Anthony S. Hartshorn, Saghar Hosseini, Rui Hou, Hakan Inan, Marcin Kardas, Viktor Kerkez, Madian Khabsa, Isabel M. Kloumann, A. V. Korenev, Punit Singh Koura, Marie-Anne Lachaux, Thibaut Lavril, Jenya Lee, Diana Liskovich, Yinghai Lu, Yuning Mao, Xavier Martinet, Todor Mihaylov, Pushkar Mishra, Igor Molybog, Yixin Nie, Andrew Poulton, Jeremy Reizenstein, Rashi Rungta, Kalyan Saladi, Alan Schelten, Ruan Silva, Eric Michael Smith, R. Subramanian, Xia Tan, Binh Tang, Ross Taylor, Adina Williams, Jian Xiang Kuan, Puxin Xu, Zhengxu Yan, Iliyan Zarov, Yuchen Zhang, Angela Fan, Melanie Kambadur, Sharan Narang, Aurelien Rodriguez, Robert Stojnic, Sergey Edunov, and Thomas Scialom. Llama 2: Open foundation and fine-tuned chat models. *ArXiv*, abs/2307.09288, 2023b. URL https://api.semanticscholar.org/CorpusID:259950998. 2

Jordy Van Landeghem, Rubèn Tito, Łukasz Borchmann, Michał Pietruszka, Pawel Joziak, Rafal Powalski, Dawid Jurkiewicz, Mickaël Coustaty, Bertrand Anckaert, Ernest Valveny, et al. Document understanding dataset and evaluation (dude). In *Proceedings of the IEEE/CVF International Conference on Computer Vision*, pp. 19528–19540, 2023. 2

Junyang Wang, Haiyang Xu, Haitao Jia, Xi Zhang, Ming Yan, Weizhou Shen, Ji Zhang, Fei Huang, and Jitao Sang. Mobile-agent-v2: Mobile device operation assistant with effective navigation via multi-agent collaboration. *arXiv preprint arXiv:2406.01014*, 2024. 2

Weihan Wang, Qingsong Lv, Wenmeng Yu, Wenyi Hong, Ji Qi, Yan Wang, Junhui Ji, Zhuoyi Yang, Lei Zhao, Xixuan Song, Jiazheng Xu, Bin Xu, Juanzi Li, Yuxiao Dong, Ming Ding, and Jie Tang. Cogvlm: Visual expert for pretrained language models. *ArXiv*, abs/2311.03079, 2023. URL https://api.semanticscholar.org/CorpusID:265034288. 7

Xin Wang, Jiawei Wu, Junkun Chen, Lei Li, Yuan-Fang Wang, and William Yang Wang. Vatex: A large-scale, high-quality multilingual dataset for video-and-language research. In *Proceedings of the IEEE/CVF international conference on computer vision*, pp. 4581–4591, 2019. 6

Haoning Wu, Dongxu Li, Bei Chen, and Junnan Li. Longvideobench: A benchmark for long-context interleaved video-language understanding. *arXiv preprint arXiv:2407.15754*, 2024. 2, 7, 21

Junbin Xiao, Xindi Shang, Angela Yao, and Tat seng Chua. Next-qa: Next phase of question-answering to explaining temporal actions. *2021 IEEE/CVF Conference on Computer Vision and Pattern Recognition (CVPR)*, pp. 9772–9781, 2021. URL https://api.semanticscholar.org/CorpusID:234763093. 2, 7, 21

Jun Xu, Tao Mei, Ting Yao, and Yong Rui. Msr-vtt: A large video description dataset for bridging video and language. In *Proceedings of the IEEE conference on computer vision and pattern recognition*, pp. 5288–5296, 2016. 6

An Yang, Baosong Yang, Binyuan Hui, Bo Zheng, Bowen Yu, Chang Zhou, Chengpeng Li, Chengyuan Li, Dayiheng Liu, Fei Huang, et al. Qwen2 technical report. *arXiv preprint arXiv:2407.10671*, 2024. 3

Jiabo Ye, Anwen Hu, Haiyang Xu, Qinghao Ye, Ming Yan, Guohai Xu, Chenliang Li, Junfeng Tian, Qi Qian, Ji Zhang, et al. Ureader: Universal ocr-free visually-situated language understanding with multimodal large language model. In *The 2023 Conference on Empirical Methods in Natural Language Processing*, 2023a. 6, 15

Qinghao Ye, Haiyang Xu, Guohai Xu, Jiabo Ye, Ming Yan, Yiyang Zhou, Junyang Wang, Anwen Hu, Pengcheng Shi, Yaya Shi, et al. mplug-owl: Modularization empowers large language models with multimodality. *arXiv preprint arXiv:2304.14178*, 2023b. 2, 10

Qinghao Ye, Haiyang Xu, Jiabo Ye, Ming Yan, Anwen Hu, Haowei Liu, Qi Qian, Ji Zhang, and Fei Huang. mplug-owl2: Revolutionizing multi-modal large language model with modality collaboration. In *Proceedings of the IEEE/CVF Conference on Computer Vision and Pattern Recognition*, pp. 13040–13051, 2024. 2, 4, 5

Weihao Yu, Zhengyuan Yang, Linjie Li, Jianfeng Wang, Kevin Lin, Zicheng Liu, Xinchao Wang, and Lijuan Wang. Mm-vet: Evaluating large multimodal models for integrated capabilities. *arXiv preprint arXiv:2308.02490*, 2023. 7, 20

Xiaohua Zhai, Basil Mustafa, Alexander Kolesnikov, and Lucas Beyer. Sigmoid loss for language image pre-training. In *Proceedings of the IEEE/CVF International Conference on Computer Vision*, pp. 11975–11986, 2023. 3

Chaoyun Zhang, Liqun Li, Shilin He, Xu Zhang, Bo Qiao, Si Qin, Minghua Ma, Yu Kang, Qingwei Lin, Saravan Rajmohan, et al. Ufo: A ui-focused agent for windows os interaction. *arXiv preprint arXiv:2402.07939*, 2024a. 2

Ruohong Zhang, Liangke Gui, Zhiqing Sun, Yihao Feng, Keyang Xu, Yuanhan Zhang, Di Fu, Chunyuan Li, Alexander Hauptmann, Yonatan Bisk, et al. Direct preference optimization of video large multimodal models from language model reward. *arXiv preprint arXiv:2404.01258*, 2024b. 6

Zicheng Zhang, Haoning Wu, Erli Zhang, Guangtao Zhai, and Weisi Lin. A benchmark for multi-modal foundation models on low-level vision: from single images to pairs. *arXiv preprint arXiv:2402.07116*, 2024c. 7, 22

Haozhe Zhao, Zefan Cai, Shuzheng Si, Xiaojian Ma, Kaikai An, Liang Chen, Zixuan Liu, Sheng Wang, Wenjuan Han, and Baobao Chang. Mmicl: Empowering vision-language model with multi-modal in-context learning. *arXiv preprint arXiv:2309.07915*, 2023. 2

Lianmin Zheng, Wei-Lin Chiang, Ying Sheng, Siyuan Zhuang, Zhanghao Wu, Yonghao Zhuang, Zi Lin, Zhuohan Li, Dacheng Li, Eric. P Xing, Hao Zhang, Joseph E. Gonzalez, and Ion Stoica. Judging llm-as-a-judge with mt-bench and chatbot arena, 2023. 2

Junjie Zhou, Yan Shu, Bo Zhao, Boya Wu, Shitao Xiao, Xi Yang, Yongping Xiong, Bo Zhang, Tiejun Huang, and Zheng Liu. Mlvu: A comprehensive benchmark for multi-task long video understanding. *arXiv preprint arXiv:2406.04264*, 2024. 7, 21

A Training Details

Stage 1: Pretraining		Stage 2: Multi-Image Training		Stage 3: Self-Supervised Fintuning	
Dataset Name	**Percentage**	**Dataset Name**	**Percentage**	**Dataset Name**	**Percentage**
DataComp-1B	35.22%	ShareGPTVideo	34.63%	LLAVA-SFT	57.95%
LAION-en	26.07%	Selective Caption	19.29%	The Cauldron	12.50%
COYO-700M	14.47%	M4-Instruction	16.69%	Mantis	10.41%
COYO-700M-OCR	9.60%	VATEX	15.77%	M4-Instruction	9.26%
LAION-zh	7.73%	Text Reading	7.36%	ALLAVA	6.95%
Wukong	5.64%	Interleaved Caption	5.25%	ShareGPTVideo-QA	2.02%
CC12M	0.81%	MMDU	1.01%	Video Instruct	0.84%
Others	0.46%	-	-	MSRTT/MSVD Caption	0.06%

Table 7: Dataset percentages used in Pretraining, Multi-Image Training, and Self-Supervised Fintuning. Others include CC3M, OCR-CC, COCO and SBU.

Setting		Stage 1: Pretraining	Stage 2: Multi-Image Training	Stage 3: Self-Supervised Fintuning
Training	Learning Rate (Max, Min)	(1e-3, 1e-5)	(2e-5, 1e-7)	(2e-5, 1e-7)
	Global Batch Size	2048	1024	1024
	Training Steps	20K	3K	11K
	Warmup ratio	0.03		
	Trainable Modules	Linear Projection Visual KV Projection Adaptive Gate	Linear Projection Full Language Model	Linear Projection Full Language Model
Model	Resolution	384^2	up to $384^2 \times 6$	up to $384^2 \times 6$
	Sequence Length	768	4096	4096
Accelerating	Precision	Mixed-precision FP16/BF16		
	ZeRO Optimization	Zero-1		
	Gradient Checkpointing	No.	Yes.	Yes.
	Model Parallel	TP=1	TP=4	TP=4

Table 8: The training settings across three stages: Pretraining, Multi-Image Training, and Self-Supervised Finetuning.

A.1 Training Data Processing

For high-resolution images, inspired by UReader (Ye et al., 2023a), we introduce a similar adaptive method for image cropping. For a given image, we select from the cropping grids (2,2), (1,3), (1,4), (3,1), (4,1), (2,3), and (3,2) that most closely matches the shape of the input image. Additionally, we retain a global version of the original image. During the Supervised-Finetuning stage, for datasets rich in text, we perform cropping with a probability of 100%. For datasets containing a single image without text, we apply cropping with a probability of 20%. For datasets containing multiple images or videos, we do not perform cropping. During evaluation, cropping is enabled only for single-image tasks.

For videos, we sample 8 frames per video by default. Meanwhile, we replace the video markers in the text with multiple <|*image*|> placeholders corresponding to the number of sampled frames.

B Fine-grained Investigation of Capabilities in Multi-image Scenarios

To more comprehensively investigate the fine-grained abilities of mPLUG-Owl3 in multi-image scenarios, we conduct experiments on MI-Bench (Liu et al., 2024b), a recently proposed multi-image benchmark. We exclude Fine-Grained Visual Recognition from evaluation because it consists of images from mini-ImageNet that may have been seen by existing models.

Table 9 shown that mPLUG-Owl3 achieves state-of-the-art performance on aspects of General Comparison, Subtle Difference, Temporal Reasoning, Logical Reasoning and Text-Rich Images across popular open-sourced MLLMs. It also outperform GPT-4V and GPT-4o on General Comparison.

Model	GC	SD	VR	TR	LR	TRI	VTK	TVK
Closed-source MLLMs								
GPT-4o	80.7	90.5	46.8	68.0	69.8	74.8	54.7	63.3
GPT-4V	72.8	79.2	45.8	61.8	66.3	71.0	52.0	56.0
Open-source MLLMs								
mPLUG-Owl2	64.2	40.1	35.6	30.7	41.3	39.0	17.0	25.6
MMICL	53.7	46.4	**41.1**	**47.0**	59.6	27.6	22.1	35.9
Idefics2-I	83.1	49.7	32.6	44.8	56.4	43.9	25.6	39.0
Mantis	83.0	54.1	37.6	45.5	63.4	37.7	26.4	41.7
mPLUG-Owl3	**86.4**	**70.1**	33.0	46.8	**67.2**	**50.1**	**34.0**	**48.8**

Table 9: **Multi-image evaluation on MI-Bench (Liu et al., 2024b)**. We use **bold** to mark the highest score of open-sourced multimodel large language models. The evaluation consists of the following tasks: General Comparison (GC), Subtle Difference (SD), Visual Referring (VR), Temporal Reasoning (TR), Logical Reasoning (LR), Text-Rich Images (TRI), Vision-linked Textual Knowledge (VTK) and Text-linked Visual Knowledge (TVK).

The results demonstrates that our model possesses robust capabilities in various multi-image input scenarios. The Hyper Attention structure of mPLUG-Owl3 better preserves the original visual features, enabling it to excel in single-image tasks as well. And this type of multimodal knowledge also assists it in more accurately completing multi-image tasks.

C Visual-link Knowledge Enhance

Based on MI-Bench, we further examine the performance in scenarios involving supplementary visual knowledge and present the results in Table 10. Specifically, we test the models' performance in the Vision-linked Textual Knowledge task under conditions with and without additional visual knowledge. Since the provided visual knowledge does not always correspond to the images related to the questions, this setup more accurately simulates the performance of models in real-world Retrieval-Augmented Generation systems. Results show that LLaVA-Interleave achieves higher accuracy without external knowledge, while noisy interleaved text and image inputs severely degrade its performance. In contrast, mPLUG-Owl3 is capable of identifying relevant visual knowledge from noisy inputs, thereby enhancing its accuracy.

Models	w/o Visual-link Knowledge	w/ Visual-link Knowledge
LLaVA-Interleave	31.2	28.7 (-2.5)
mPLUG-Owl3	32.1	34.0 (+1.9)

Table 10: Visual-link Knowledge Enhance experiment between LLaVA-Interleave and mPLUG-Owl3.

D Distractor Resistance in Long Visual Contexts

We notice that multimodal models, when modeling multiple images, are susceptible to interference from surrounding images, leading to visual illusions. Therefore, we develop a challenge evaluation method to assess the distractor resistance of multimodal models in long visual contexts.

Specifically, we take samples from the MMBench dev set. For each test sample, we randomly select $N - 1$ images from the original MMBench dev set as distractor and construct the model input in the format of *Image 1: <|image|> Image 2: <|image|> ... Image N: <|image|>. In Image X, {question}*, where $N = 1, 5, 10, 20, 50, 100, 200, 400$ and X denotes the index of the image corresponding to the question. We use the CircularEval to measure the accuracy scores. For each question, we construct test samples with different orders of options and varying distractor images. The model needs to

Hyper Attention Layers Indices	GQA	TextVQA	MvBench	VideoMME	NLVR2	Mantis-Eval
$[9, 27]$	55.1	**51.3**	42.2	38.2	58.3	48.4
$[1, 5, 9, 13, 17, 21, 25, 29]$	56.2	48.3	41.5	**39.5**	52.4	47.5
$[1, 9, 17, 25]$	**57.6**	50.0	**42.8**	39.4	**59.5**	**51.6**

Table 11: Comparison between different layers for integrating hyper attention structures. We use **bold** to mark the highest score.

answer all test samples for a given question correctly for it to be counted as correct. Consequently, as the number of distractor images increases, the evaluation becomes significantly more challenging.

The results are shown in Figure 4. It can be observed that the introduction of distractor images results in a certain degree of performance loss for all the models. When the number of images reaches 20 and 50, the performance of LLaVA-Next-Interleave dramatically drops to 43.18% and 12.52%, respectively. We observe that when the number of images reaches 50, LLaVA struggles to consistently answer the questions accurately when different distractor images are present, resulting in a low accuracy rate. And when the number of images reaches 100, Mantis-Idefics2 fails to solve most of the problems correctly. In contrast, mPLUG-Owl3 only drops to a performance level of 43.09% when processing 50 images. As the number of images increases to 400, the performance of mPLUG-Owl3 decreases to 28.58%. Since our multi-image training data consists of only about 6-8 images, this also presents a challenge for our model. Nonetheless, mPLUG-Owl3 can serve as a baseline for future research.

E Impact of Integration Density of Hyper Attention

We explore the integration density of the hyper attention. As shown in Table 11 the results indicate that even with just two layers of Hyper Attention, the model achieves impressive performance on single-image benchmarks, while also demonstrating generalization capabilities for videos and multiple images. However, when we apply a denser integration strategy by introducing eight layers of Hyper Attention, we find that it does not yield improved single-image performance at this scale of training data, and its zero-shot generalization is even worse. Therefore, we ultimately integrate only four layers into the entire model.

F Performance of Small-sized Models

Small-scale language models can be more easily deployed on the edge, and mPLUG-Owl3 can further enhance the efficiency of these smaller language models on multimodal scenario. We provide the performance of mPLUG-Owl3 based on 0.5B and 1.5B language models across single-image, video, and multi-image understanding tasks in Table 1, Table 2, Table 3 and Table 4. The results indicate that for single-image understanding, the 1B and 2B models exhibit an average performance drop of 19.1% and 6.7% compared to the 8B model. Meanwhile, we notice that the 2B-sized model achieving performance comparable to LLaVA-Next 8B. In the video domain, we find that the smaller models do not suffer much performance loss (averaging 10.5% and 3.5%); even the mPLUG-Owl3 2B outperforms the 8B scale model on long video understanding tasks. However, in multi-image understanding tasks, we observe a more significant performance drop for the smaller models, with the 1B and 2B models showing declines of 28.8% and 18%, respectively. This is because understanding relationships among multiple images is more reliant on the capabilities of the language model.

G Qualitative Results

mPLUG-Owl3 can handle various number of images and videos as inputs. In this section, we further investigate the ability of mPLUG-Owl3 in real-world dialogue scenarios.

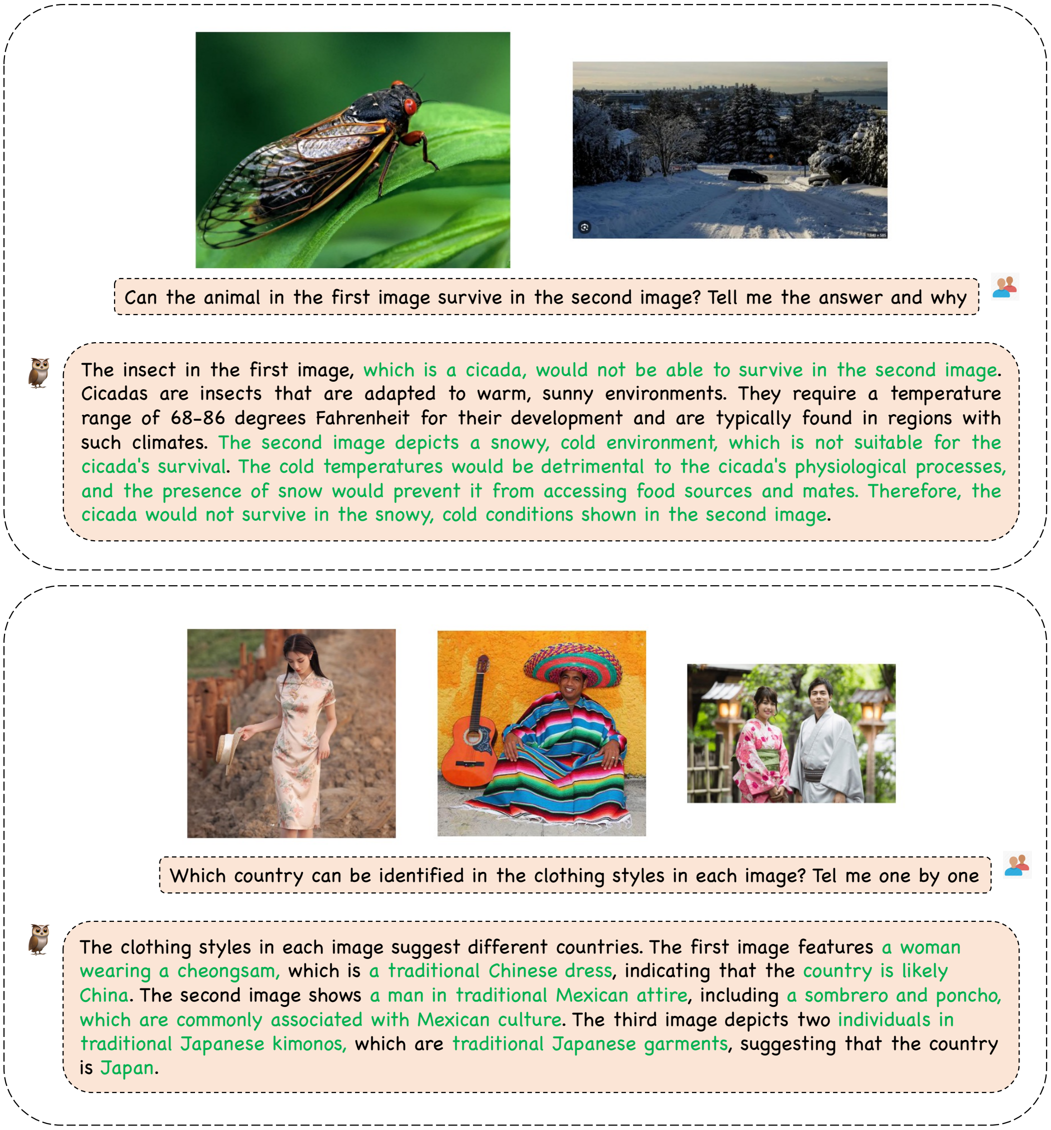

Can the animal in the first image survive in the second image? Tell me the answer and why

The insect in the first image, which is a cicada, would not be able to survive in the second image. Cicadas are insects that are adapted to warm, sunny environments. They require a temperature range of 68-86 degrees Fahrenheit for their development and are typically found in regions with such climates. The second image depicts a snowy, cold environment, which is not suitable for the cicada's survival. The cold temperatures would be detrimental to the cicada's physiological processes, and the presence of snow would prevent it from accessing food sources and mates. Therefore, the cicada would not survive in the snowy, cold conditions shown in the second image.

Which country can be identified in the clothing styles in each image? Tel me one by one

The clothing styles in each image suggest different countries. The first image features a woman wearing a cheongsam, which is a traditional Chinese dress, indicating that the country is likely China. The second image shows a man in traditional Mexican attire, including a sombrero and poncho, which are commonly associated with Mexican culture. The third image depicts two individuals in traditional Japanese kimonos, which are traditional Japanese garments, suggesting that the country is Japan.

Figure 5: Examples for Multi-Image Understanding. We highlight the correct answers in green.

G.1 Multi-Image Understanding

mPLUG-Owl3 demonstrate state-of-the-art performance on multi-image understanding benchmarks. In this section, we present multi-image dialogue examples in real-world. In the first example shown in Figure 5, it can be observed that mPLUG-Owl3 can activate the knowledge it learned based on the content of the images and perform cross-image reasoning. The second example demonstrates that the model can accurately distinguish the content of multiple images and respond appropriately based on cultural knowledge.

Figure 6 shows a multi-turn dialogue example. mPLUG-Owl3 can find the differences between two images in various views. Besides, it can describe the correlations between images.

As shown in Figure 7, mPLUG-Owl3 can maintain continuous interaction with a smartphone. During this process, the model effectively understands the multimodal interaction history and makes accurate decisions using a chain-of-thought approach. Additionally, it retains the initial user instructions without any degradation throughout the interaction.

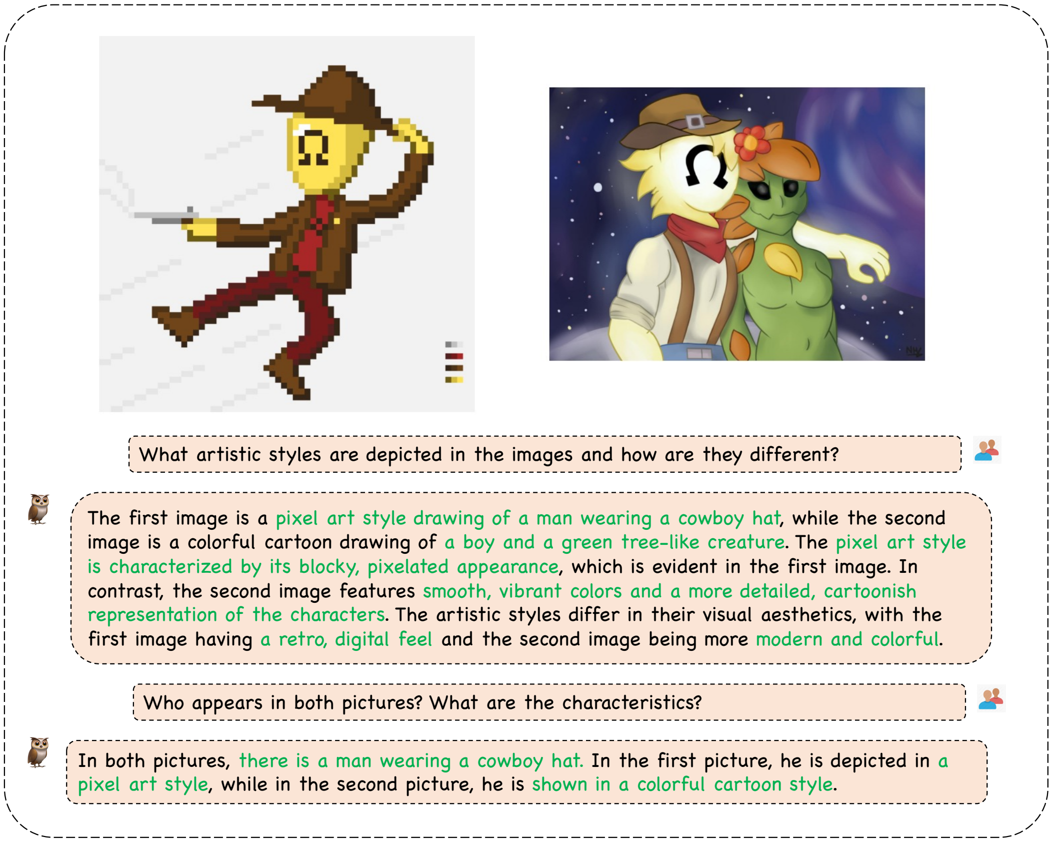

What artistic styles are depicted in the images and how are they different?

The first image is a pixel art style drawing of a man wearing a cowboy hat, while the second image is a colorful cartoon drawing of a boy and a green tree-like creature. The pixel art style is characterized by its blocky, pixelated appearance, which is evident in the first image. In contrast, the second image features smooth, vibrant colors and a more detailed, cartoonish representation of the characters. The artistic styles differ in their visual aesthetics, with the first image having a retro, digital feel and the second image being more modern and colorful.

Who appears in both pictures? What are the characteristics?

In both pictures, there is a man wearing a cowboy hat. In the first picture, he is depicted in a pixel art style, while in the second picture, he is shown in a colorful cartoon style.

Figure 6: Examples for Multi-turn Multi-Image Dialogue. We highlight the correct answers in green.

G.2 Video Understanding

We showcase the video understanding capabilities of mPLUG-Owl3. First, we compare it with LLaVA-Next-Interleave in Short Video Question Answering, Long Video Fine-grained Question Answering, and Long Video Comprehensive Understanding. For LLaVA-Next-Interleave, we input 8 frames, while for mPLUG-Owl3, we input 128 frames, which are the maximum numbers of images that can be accommodated by the two models on a V100-32G. The samples are shown in Figure 8.

In the short video tests, both LLaVA and mPLUG-Owl3 can provide correct answers. mPLUG-Owl3 tends to describe the attributes of objects based on the actual content seen. In long video lasting more than 40 minutes, when we ask about a specific detail, LLaVA fails to handle the long sequence and loses fine-grained information, rendering it unable to provide accurate information. On the other hand, mPLUG-Owl3 accurately captures key segment information within a long video. Additional, we have both models summarize the content of a longer video. mPLUG-Owl3's response is very detailed, not only providing an overall summary but also introducing the process in order. LLaVA-Next-Interleave's response, however, is more general and lacks detail. The comparative results indicate that mPLUG-Owl3 not only efficiently encodes long visual sequences but also captures and effectively utilizes both global and local information.

We also test mPLUG-Owl3 in multiple rounds using a long video that featuring many scenes. For clarity, we place the relevant segments beside the dialogue in the figure. During the test, we input only the complete video to the model. The dialogue is shown in Figure 9.

First, we ask a question with a temporal constraint, and mPLUG-Owl3 accurately understands the concept of "at first" and correctly describes the detail of “sitting in a room and discussing something on their laptops.” However, the response incorrectly counts the number of people. The segment has only two people. We find that the model is confused by a later scene involving more people. We

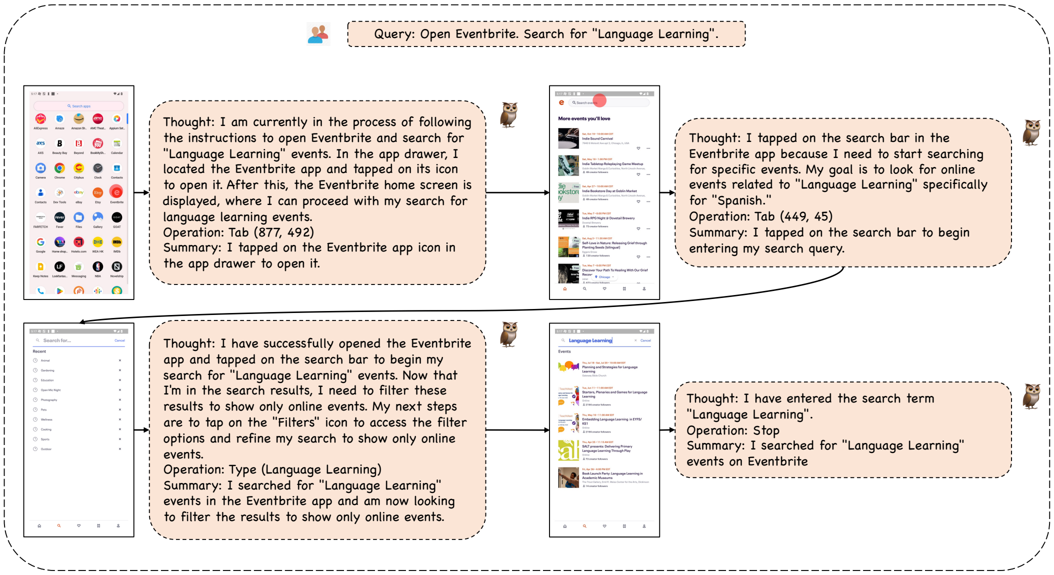

Query: Open Eventbrite. Search for "Language Learning".

Thought: I am currently in the process of following the instructions to open Eventbrite and search for "Language Learning" events. In the app drawer, I located the Eventbrite app and tapped on its icon to open it. After this, the Eventbrite home screen is displayed, where I can proceed with my search for language learning events.
Operation: Tab (877, 492)
Summary: I tapped on the Eventbrite app icon in the app drawer to open it.

Thought: I tapped on the search bar in the Eventbrite app because I need to start searching for specific events. My goal is to look for online events related to "Language Learning" specifically for "Spanish."
Operation: Tab (449, 45)
Summary: I tapped on the search bar to begin entering my search query.

Thought: I have successfully opened the Eventbrite app and tapped on the search bar to begin my search for "Language Learning" events. Now that I'm in the search results, I need to filter these results to show only online events. My next steps are to tap on the "Filters" icon to access the filter options and refine my search to show only online events.
Operation: Type (Language Learning)
Summary: I searched for "Language Learning" events in the Eventbrite app and am now looking to filter the results to show only online events.

Thought: I have entered the search term "Language Learning".
Operation: Stop
Summary: I searched for "Language Learning" events on Eventbrite

Figure 7: Example of multi-image understanding interactions between mPLUG-Owl3 and the smartphone GUI in multi-round interactions. The tap operation is annotated by a red sphere.

also notice that the visual content of this segment does not involve Australia as a destination, but the model can infer this from some diagrams later in the video, which makes the response more detailed. Then, we ask about the camera brand in a frame that briefly appears, and mPLUG-Owl3 accurately notices the "Canon" logo in the image and provides the correct answer. Finally, we ask the model to describe the travel in order of time. We use the same color to identify the content described by the model and the corresponding video segments. Since the video involves many scenes and events, this poses a great challenge to the model. It can be observed that mPLUG-Owl3 accurately details the travel according to the timeline of the video. However, we also notice that mPLUG-Owl3 exhibits some hallucinations, incorrectly interpreting the reefs captured in the video as a beach. Additionally, while the activities on the boat happen during the day, mPLUG-Owl3, influenced by other nighttime scenes, makes an incorrect statement.

H Evaluation Benchmarks

H.1 Single-image Benchmakrs

We conduct experiments on a diverse set of visual question answering benchmarks, including VQAv2 (Goyal et al., 2016), OK-VQA (Marino et al., 2019), GQA (Hudson & Manning, 2019), VizWizQA (Bigham et al., 2010), and TextVQA (Singh et al., 2019). The VQAv2 dataset is currently the largest visual question answering dataset available. OK-VQA involves questions that require external knowledge beyond multimodal inputs. GQA is designed to validate the model's reasoning capabilities. VizWizQA is constructed from question-answer pairs sourced from visually impaired users. TextVQA focuses more on evaluating the model's ability to understand text in natural scenes.

We also evaluate mPLUG-Owl3 on various single-image general multimodal large language model benchmarks. MMBench (Liu et al., 2023b) provides a comprehensive evaluation of a model's multimodal capabilities in both Chinese and English contexts. MM-Vet (Yu et al., 2023) assesses the multimodal conversational abilities of a model using GPT-4 evaluation. POPE (Li et al., 2023d) can evaluate the extent of multimodal hallucinations in a model. AI2D (Kembhavi et al., 2016) assesses a model's ability to understand science diagrams inputs.

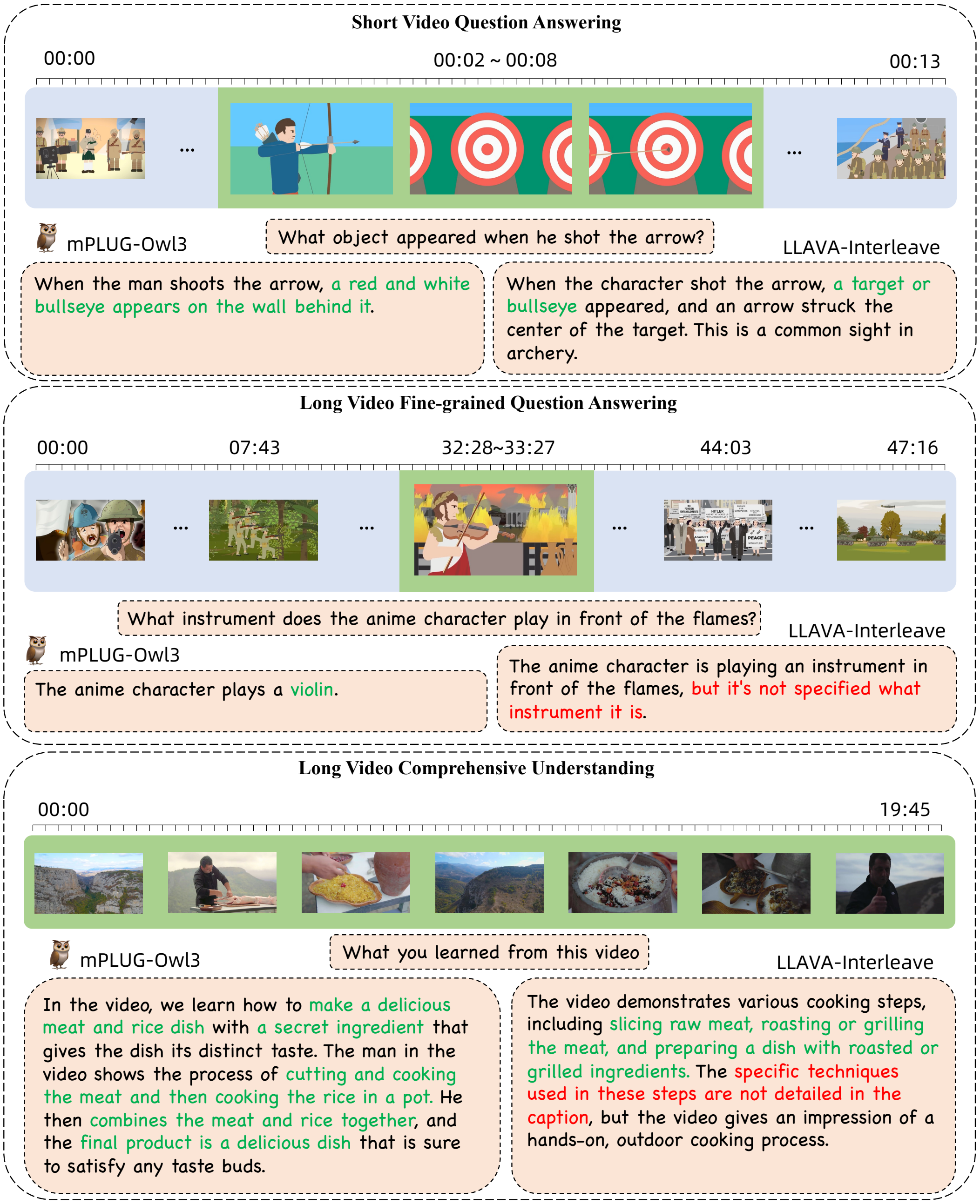

What object appeared when he shot the arrow?

When the man shoots the arrow, a red and white bullseye appears on the wall behind it.

When the character shot the arrow, a target or bullseye appeared, and an arrow struck the center of the target. This is a common sight in archery.

What instrument does the anime character play in front of the flames?

The anime character plays a violin.

The anime character is playing an instrument in front of the flames, but it's not specified what instrument it is.

What you learned from this video

In the video, we learn how to make a delicious meat and rice dish with a secret ingredient that gives the dish its distinct taste. The man in the video shows the process of cutting and cooking the meat and then cooking the rice in a pot. He then combines the meat and rice together, and the final product is a delicious dish that is sure to satisfy any taste buds.

The video demonstrates various cooking steps, including slicing raw meat, roasting or grilling the meat, and preparing a dish with roasted or grilled ingredients. The specific techniques used in these steps are not detailed in the caption, but the video gives an impression of a hands-on, outdoor cooking process.

Figure 8: Comparison between mPLUG-Owl3 and LLaVA-Interleave across Short Video Question Answering, Long Video Fine-grained Question Answering, and Long Video Comprehensive Understanding. We highlight the correct and relevant parts of the answers in green, while the parts that fail to answer the question correctly are marked in red. Additionally, the segments of the video that are relevant to the questions are highlighted with a green background.

H.2 Video Benchmarks

We conduct experiments on a diverse set of video understanding benchmarks, including NextQA (Xiao et al., 2021) and MVBench (Li et al., 2023c), which are short video benchmarks with video durations all less than one minute. Thus, we sample 8 frames and 16 frames, separately. For benchmarks like VideoMME (Fu et al., 2024a), LongVideoBench (Wu et al., 2024), and MLVU (Zhou et al., 2024), which involve longer video durations up to one hour. For , we

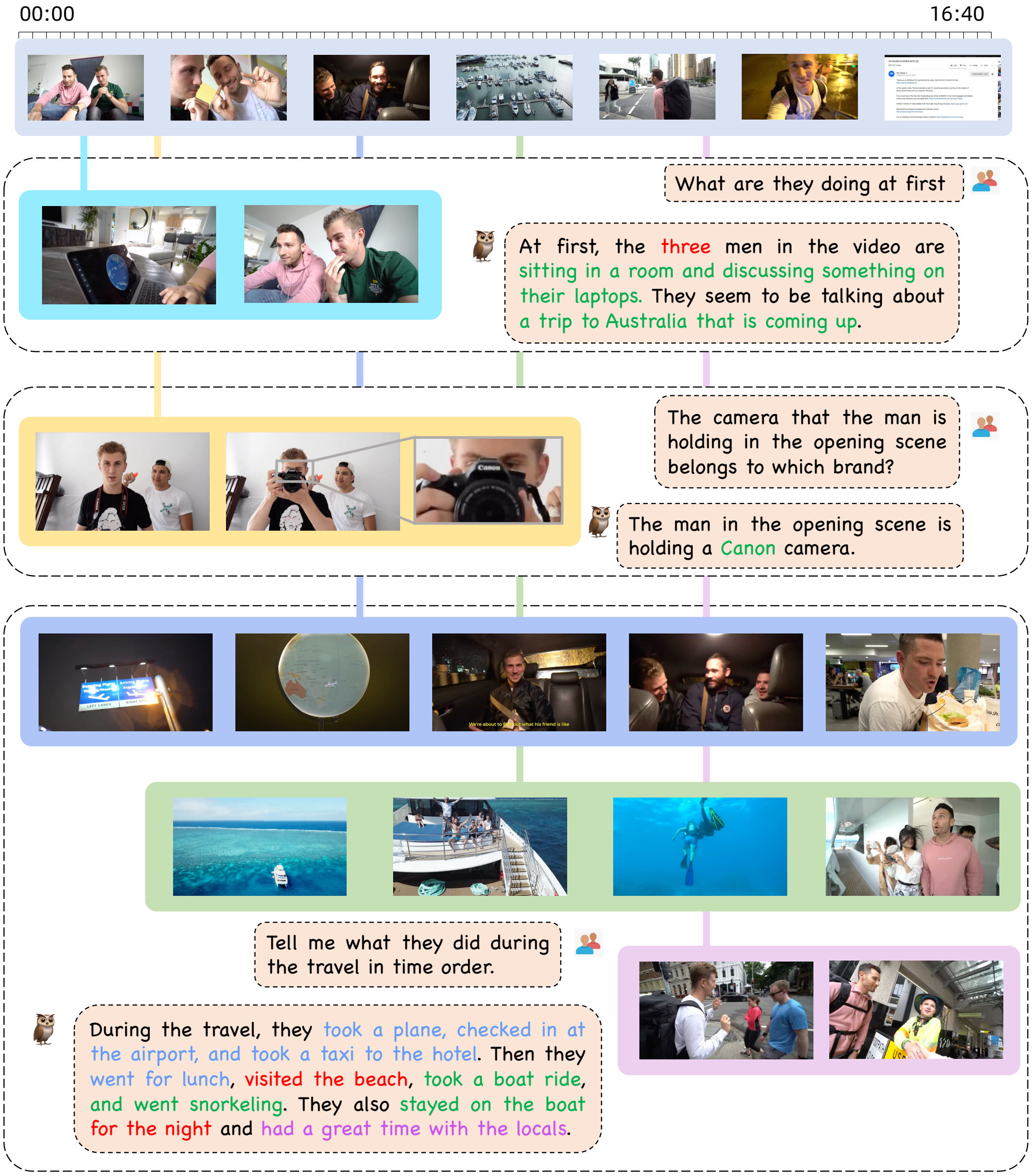

What are they doing at first

At first, the three men in the video are sitting in a room and discussing something on their laptops. They seem to be talking about a trip to Australia that is coming up.

The camera that the man is holding in the opening scene belongs to which brand?

The man in the opening scene is holding a Canon camera.

Tell me what they did during the travel in time order.

During the travel, they took a plane, checked in at the airport, and took a taxi to the hotel. Then they went for lunch, visited the beach, took a boat ride, and went snorkeling. They also stayed on the boat for the night and had a great time with the locals.

Figure 9: Examples of mPLUG-Owl3's understanding of complex video content

H.3 Multi-images Benchmarks

We conduct experiments on a diverse set of multi-image reasoning benchmarks, including NLVR2 (Suhr et al., 2018), Mantis-Eval (Jiang et al., 2024), MathVerse-mv (Li et al., 2024), SciVerse-mv (Li et al., 2024), BLINK (Fu et al., 2024b), and Q-Bench2 (Zhang et al., 2024c). NLVR2 tests the model's ability to perform logical reasoning based on the content of multiple images. Mantis-Eval evaluates the model's reasoning skills in complex scenarios involving multiple images. MathVerse-mv and SciVerse-mv assess the model's multi-image mathematical and scientific capabilities. We use the version released by llava-next-interleave for comparison with its reported results. BLINK and Q-Bench2 test the model's multi-image ability based on low-level visual perception.